CO_2 reduction to formic acid at low overpotential on BDD electrodes modified with nanostructured CeO_2

Enrico Verlato [a,b] *, Simona Barison [a], Yasuaki Einaga [c] , Marco Musiani [a], Lucia Nasi [d], Keisuke Natsui [c], Francesco Paolucci [a,b], Giovanni Valenti [c].

a: CNR-ICMATE, Corso Stati Uniti 4, 35127 Padova, Italy

b: Dept. of Chemistry G. Ciamician, University of Bologna, via Selmi 2, 40126 Bologna, Italy

c: Department of Chemistry, Keio University, 3-14-1 Hiyoshi, Yokohama 223-8522, Japan

d: CNR-IMEM, Parco Area delle Scienze 37/A, 43124 Parma, Italy

Supplementary information

[1] Details on BDD electrodes and their surface preparation, including **Fig. S1** and **Fig. S2** (Cyclic voltammetries performed on a BDD electrode in $HClO_4$ 0.1M).

[2] Description of the electrochemical cell used to study CO_2 reduction including **Fig. S3**.

Fig. S4. SEM cross sectional images of (a) bare BDD electrode, (b) CeO_2-BDD electrodes obtained at E_{dep} = -2.0V vs SCE, Q_{dep} = -1C/cm^2.

Fig. S5. XRD spectra of a CeO_2/GC electrode.

Fig. S6. XPS high-resolution measurements and spectral fits of the O1s.

Fig. S7. (a) LSV recorded with a CeO_2-BDD electrode in 0.1M phosphate buffer solution saturated with either CO_2 or N_2; scan rate 1 mVs^{-1}. (b) CV recorded with a CeO_2-BDD electrode in 0.1M $KHCO_3$; scan rate of 10 mV s^{-1}.

Fig. S8. Chronoamperograms registered during CO_2 reduction at E=-0.44V vs SHE in a CO_2 saturated 0.1M $KHCO_3$ solution on CeO_2-BDD electrodes prepared at E_{dep}=-1.0 V, Q_{dep}=-0.02 C/cm^2 (black) and E_{dep} = -2.0 V, Q_{dep}= -0.4 C/cm^2 (blue).

[1] Details on BDD electrodes and their surface preparation. BDD films were deposited on Si wafer through a microwave plasma-assisted chemical vapour deposition (CVD). They consisted of crystals with 5 μm average dimension and a range from 1 to 8 μm (Fig. S1) and were doped with 1% Boron. Increasing boron content increases conductivity but also gives higher background current and a narrower potential window. 1% of Boron corresponds to a concentration of ca 1.7 x 10^{21} boron atoms per cm^3, and is sufficient to impart BDD metal-like conduction [J.-P. Lagrange, A. Deneuville, E. Gheeraert, Activation energy in low compensated homoepitaxial boron-doped diamond films, Diamond and Related Materials 7 (1998) 1390–1393].

Cleaning of the electrodes was performed by scanning at 0.3 V/s in $HClO_4$ 0.1M for 20 cycles. Fig. S2 shows cyclic voltammetries performed to clean the electrode; the insert highlights a region that shows an oxidation peak generated by oxidation of sp^2 carbon defects. The intensity of this peak provides indications on the BDD quality in terms of carbon purity. Carbon sp^2 impurities in the BDD film are often considered to be the active sites for electrochemical reactions, albeit they are responsible of decreasing the stability of electrode surface and reducing free potential window.

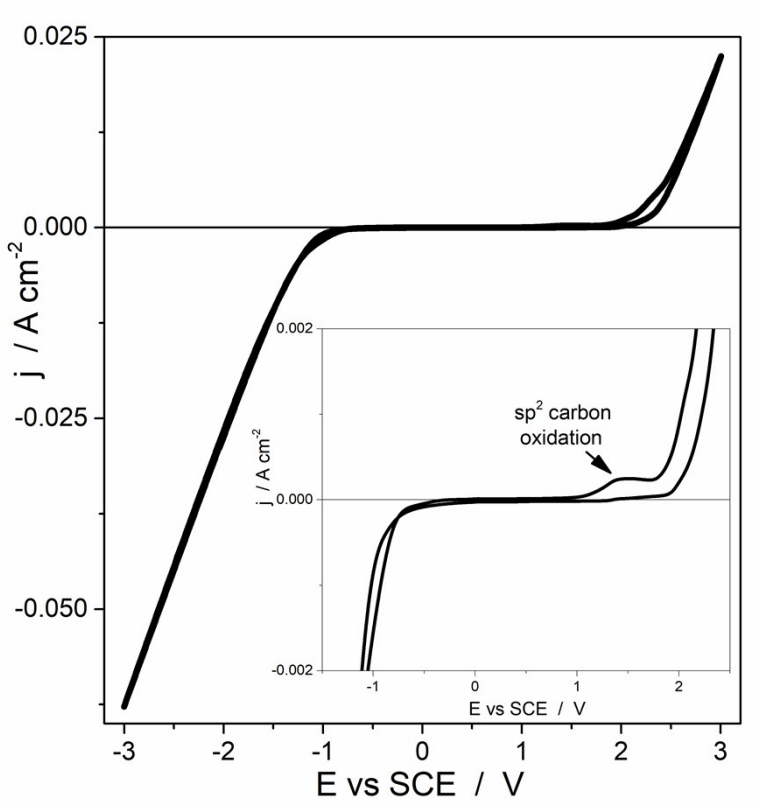

Fig. S1. Cyclic voltammetry performed on a BDD electrode in $HClO_4$ 0.1M, scan rate 0.300 V s^{-1}, 20 cycles. Zoom of the potential window with carbon sp^2 oxidation peak.

Surface termination of BDD is an important parameter, because it influences electron transfer kinetics and wettability of the electrode. Before any experiment, after cleaning, we performed a surface

activation by cycling the electrode between 0 an -3V vs SCE in $HClO_4$ to restore H-termination. For our electrochemical measurements, that include cathodic scans and polarizations, having a H-termination was mandatory to maintain a good reproducibility. Fig. S3 shows H-termination restoring evidenced by hydrogen evolution current increasing toward cycling.

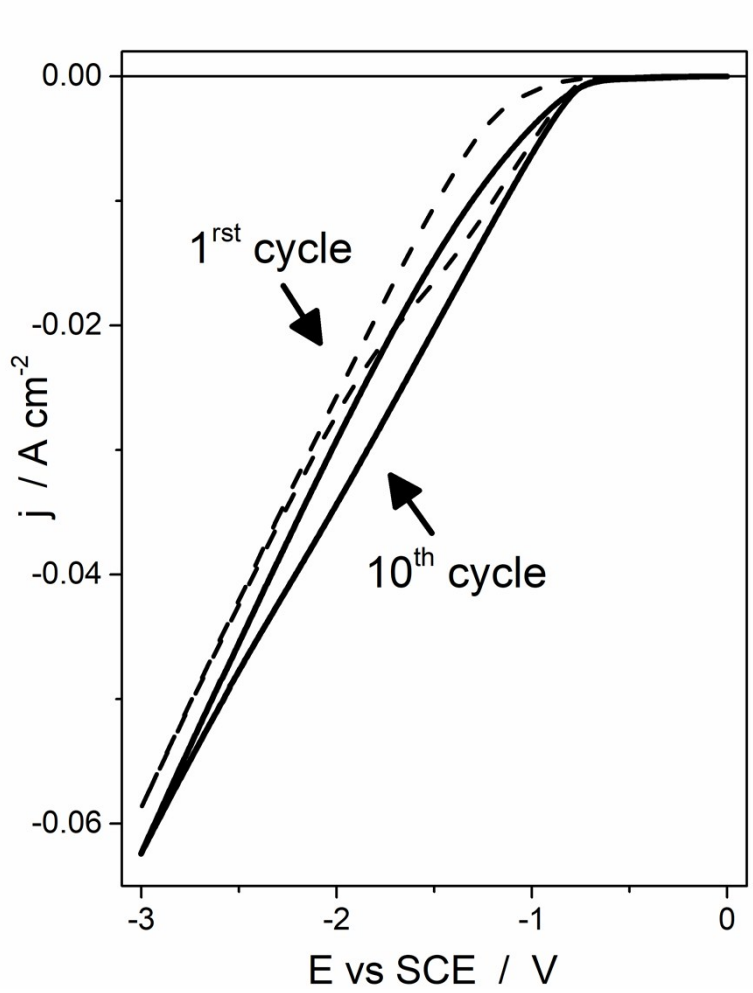

Fig. S2. Cyclic voltammetry performed on a BDD electrode in $HClO_4$ 0.1M, scan rate 0.300 V/s, 1^{rst} and 10th cycles reported.

[2] Electrolysis were performed in a custom-made three electrodes electrochemical cell specifically designed and realized in the facilities of the "Centre de Recherche Paul Pascal" (CRPP) in Pessac (France) thanks to a long-standing collaboration between the EMFM group in Bologna and the research group of Dr. Alain Penicaud in that institution.

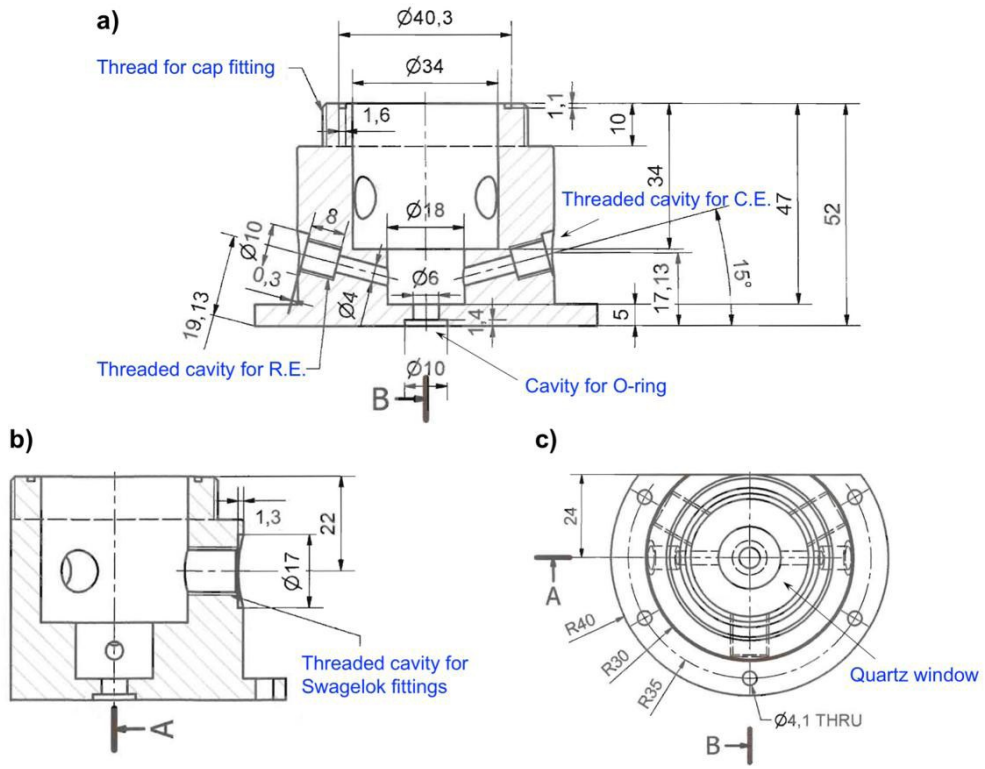

Figure S3: Front, **a)** , lateral **b)** and top **c)** views of the electrochemical cell**. d)** 3D rendering of the electrochemical cell, with highlighted the main components. The working electrode is not visible, but the interchangeable basal plate can accommodate planar SPE as well as rod-like electrodes with Ø = 6 mm. The drawings are not in scale.

As can be seen in Fig. **S3**, the cell presents two threaded cavities near the bottom of the main body, where the R.E. and the C.E. can be accommodated. Both electrodes are placed into glass tubes and isolated from the electrolytic solution with medium size porous frits. To ensure the gas-tightness at the electrode-cell body junction, Teflon or Viton O-rings are placed around the glass tubes and fitted into PEEK nut connectors (Upchurch Scientific Ltd.) which are screwed directly into the body of the cell. A peculiar characteristic of the cell is also the bottom part, that consists of circular interchangeable adapters into which different W.E. can be placed. These adapters are tightened with 6 screws to the main body and allow to use different W.E. with different geometries. In this work only BDD or GC sheet electrodes have been used, but commercial SPEs and in general plane electrodes, can be used as well. The top of the cell is closed with a cap that is screwed on the main body. Two Viton sealings are placed between the cell and the cap to avoid the escape of gases. Connection with the gas line from the cylinders (N_2 or CO_2) is assured by two Swagelok stainless steel connectors that in this case are screwed into the main body and have Viton O-rings to prevent gas leaks.

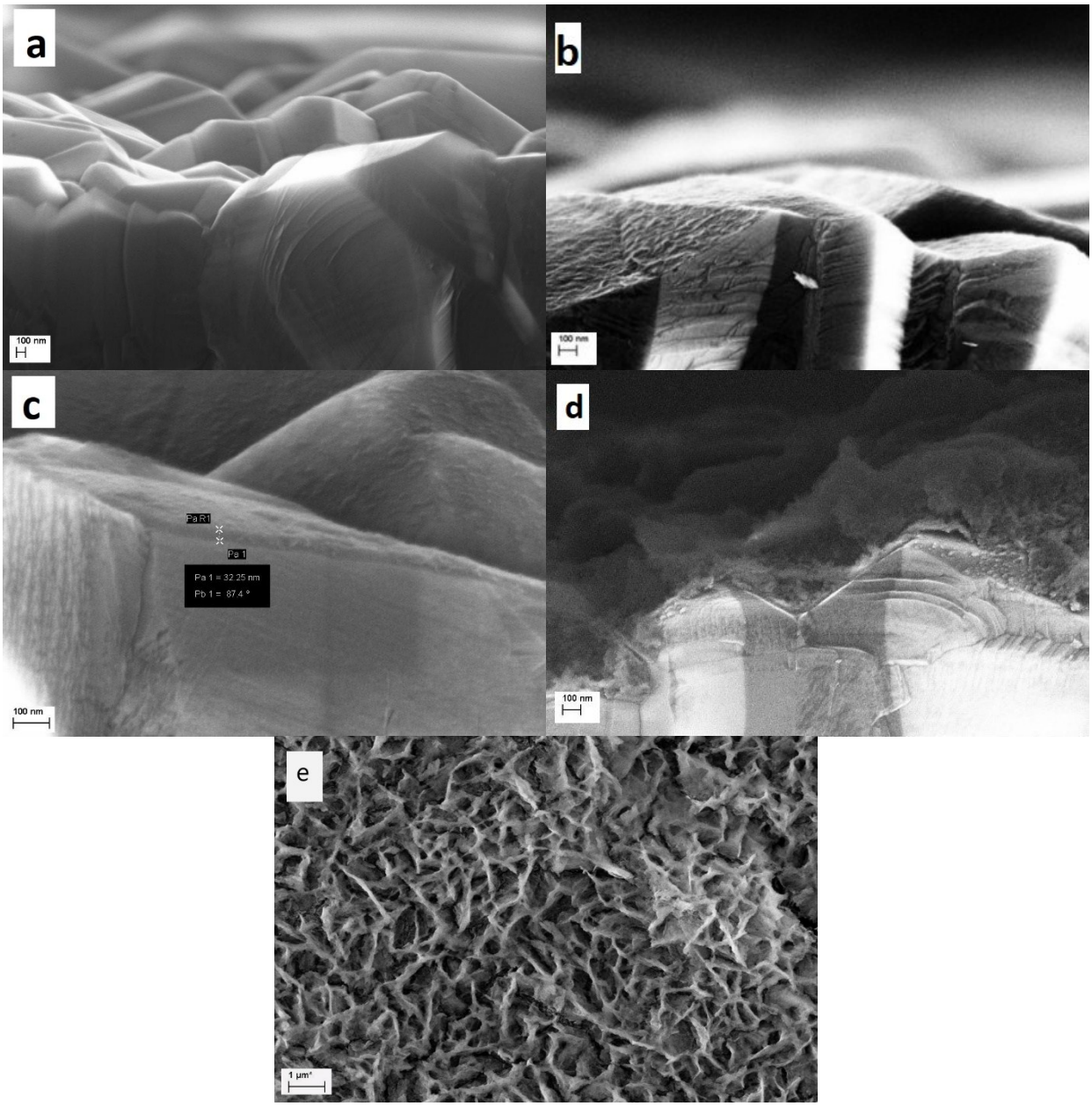

Fig. S4. SEM cross sectional images of (a) bare BDD electrode, (b) CeO_2-BDD electrode obtained at E_{dep} = -1.0 V vs SCE, Q_{dep} = -0.02 C/cm^2, (c) CeO_2-BDD electrode obtained at E_{dep} = -2.0 V vs SCE, Q_{dep} = -1 C/cm^2 (d) CeO_2-BDD electrode obtained at E_{dep} = -1.0 V vs SCE, Q_{dep} = -0.2 C/cm^2. (e) top view of a CeO_2-BDD electrode obtained at E_{dep} = -1.0 V vs SCE, Q_{dep} = -0.5 C/cm^2.

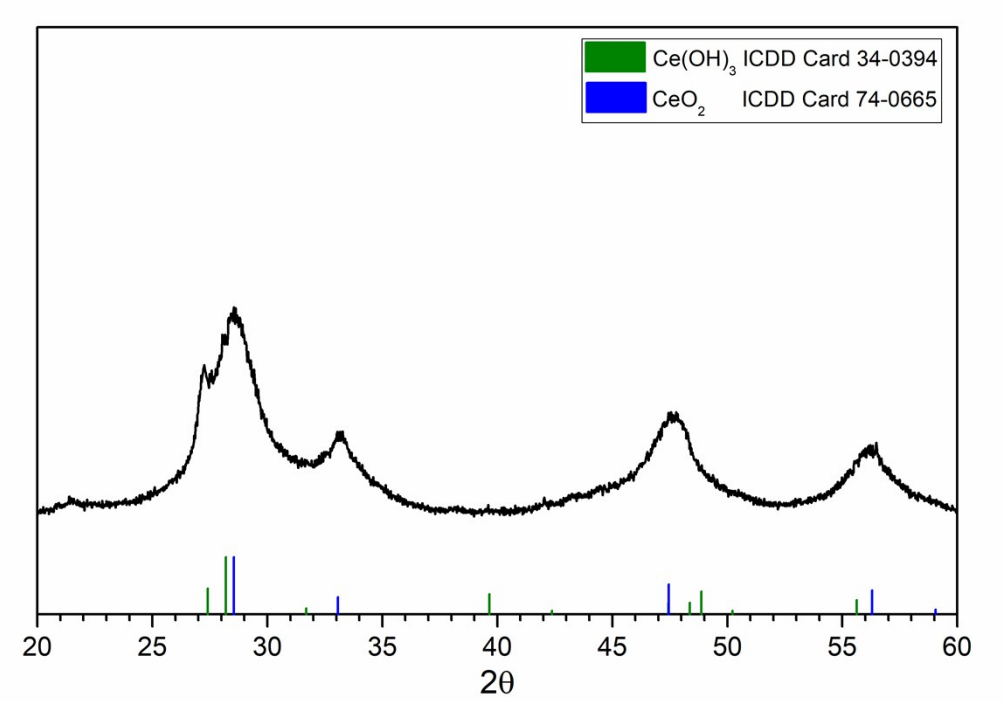

Fig. S5. XRD spectra of a CeO_2/GC electrode obtained with the same deposition current and charge of CeO_2/BDD electrode used for CO_2RR.

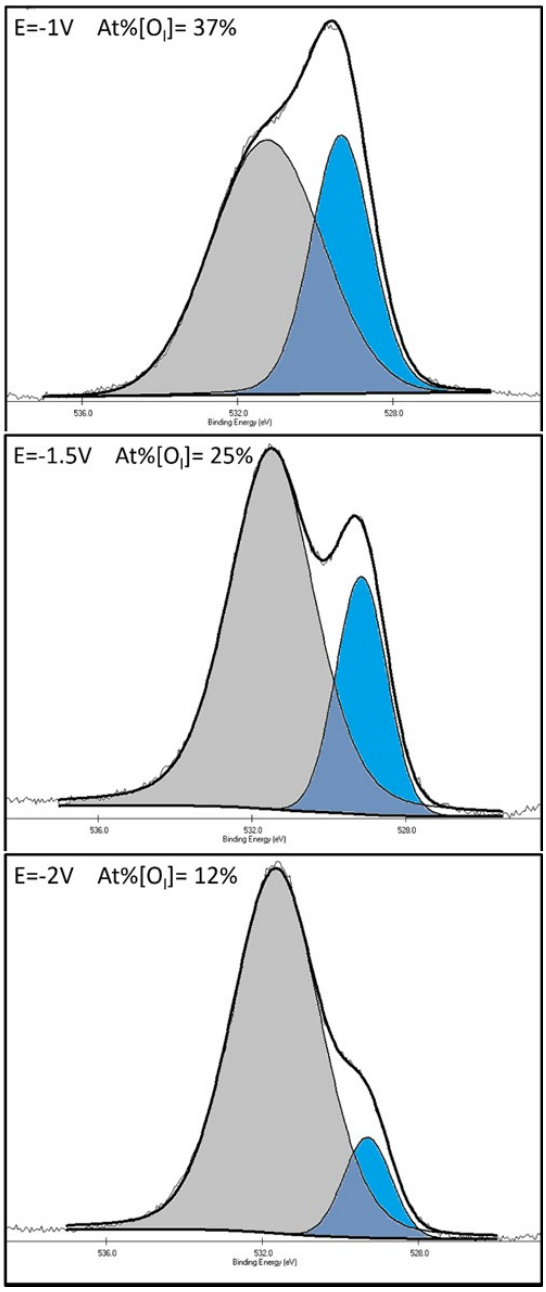

Fig. S6. XPS high-resolution measurements and spectral fits of the O1s.

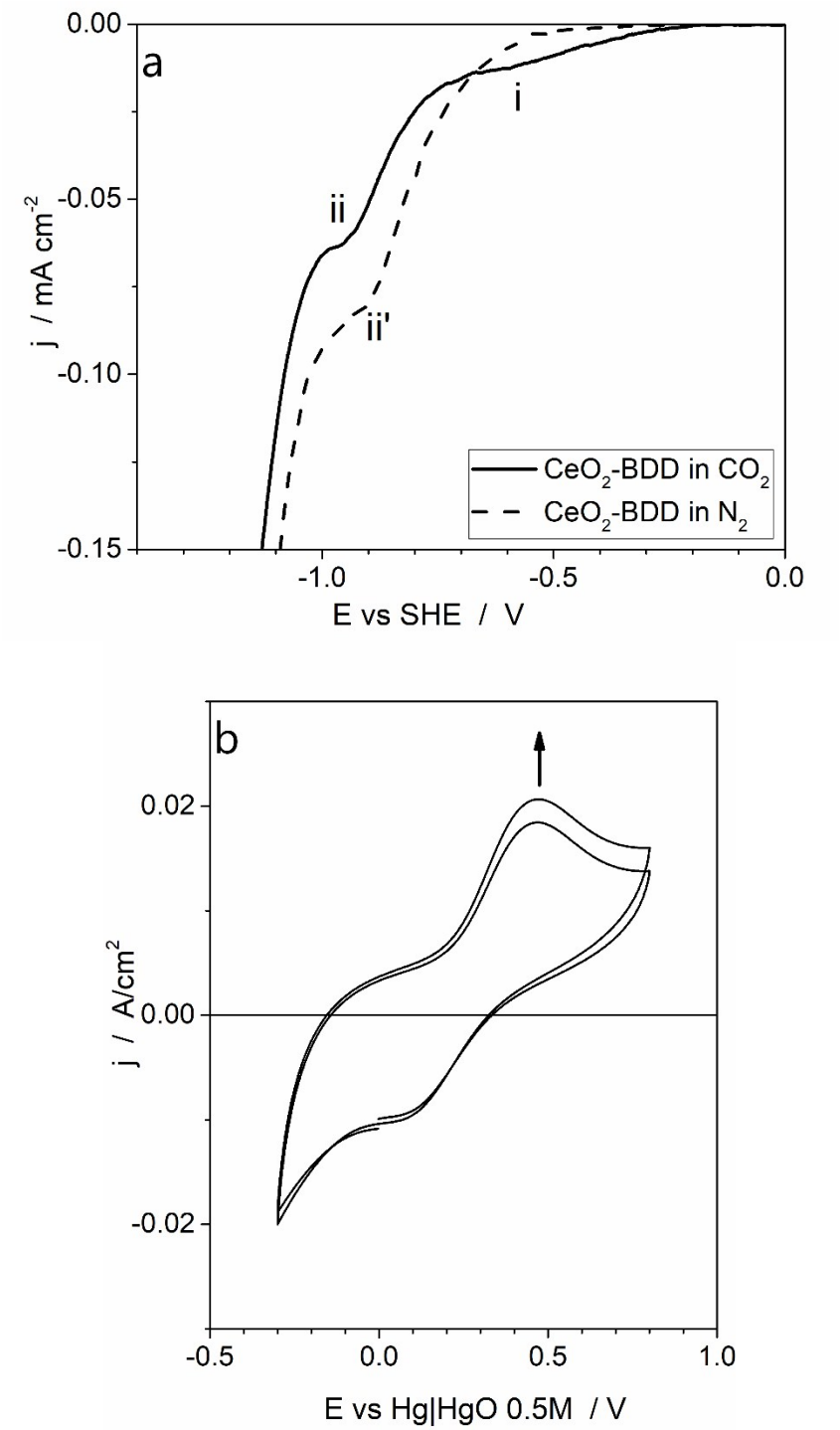

Fig. S7. (a) LSV recorded with a CeO_2-BDD electrode in 0.1M phosphate buffer solution saturated with either CO_2 or N_2; scan rate 1 mVs^{-1}. (b) CV recorded with a CeO_2-BDD electrode in 0.1M $KHCO_3$; scan rate of 10 mV s^{-1}.

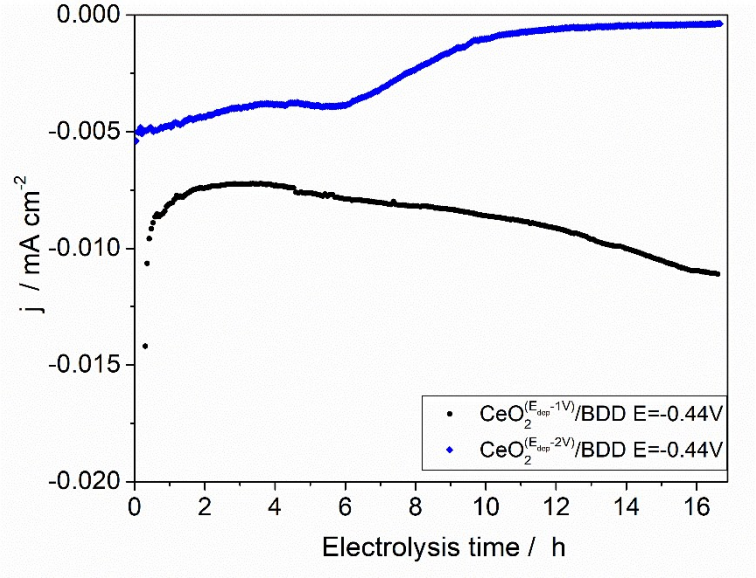

Fig. S8. Chronoamperograms registered during CO_2 reduction at E=-0.44V vs SHE in a CO_2 saturated 0.1M $KHCO_3$ solution on CeO_2-BDD electrodes prepared at E_{dep}=-1.0 V, Q_{dep}=- 0.02 C/cm^2 (black) and E_{dep} = -2.0 V, Q_{dep}= -0.4 C/cm^2 (blue).